International Journal of Radiation Oncology biology • physics

www.redjournal.org

Physics Contribution

Initial Clinical Experience of Cherenkov Imaging in External Beam Radiation Therapy Identifies Opportunities to Improve Treatment Delivery

Lesley A. Jarvis, MD, PhD,* Rachael L. Hachadorian, MS,† Michael Jermyn, PhD,† Petr Bruza, PhD,† Daniel A. Alexander, MS,† Irwin I. Tendler, PhD,† Benjamin B. Williams, PhD,*,† David J. Gladstone, ScD,*,† Philip E. Schaner, MD, PhD,* Bassem I. Zaki, MD,* and Brian W. Pogue, PhD†

Department of Medicine, Section of Radiation Oncology, Geisel School of Medicine at Dartmouth, Hanover, New Hampshire; and †Thayer School of Engineering at Dartmouth, Hanover, New Hampshire

Received Jun 5, 2020. Accepted for publication Nov 5, 2020.

Purpose: The value of Cherenkov imaging as an on-patient, real-time, treatment delivery verification system was examined in a 64-patient cohort during routine radiation treatments in a single-center study.

Methods and Materials: Cherenkov cameras were mounted in treatment rooms and used to image patients during their standard radiation therapy regimen for various sites, predominantly for whole breast and total skin electron therapy. For most patients, multiple fractions were imaged, with some involving bolus or scintillators on the skin. Measures of repeatability were calculated with a mean distance to conformity (MDC) for breast irradiation images.

Results: In breast treatments, Cherenkov images identified fractions when treatment delivery resulted in dose on the contralateral breast, the arm, or the chin and found nonideal bolus positioning. In sarcoma treatments, safe positioning of the contralateral leg was monitored. For all 199 imaged breast treatment fields, the interfraction MDC was within 7 mm compared with the first day of treatment (with only 7.5% of treatments exceeding 3 mm), and all but 1 fell within 7 mm relative to the treatment plan. The value of imaging dose through clear bolus or quantifying surface dose with scintillator dots was examined. Cherenkov imaging also was able to assess field match lines in cerebral-spinal and breast irradiation with nodes. Treatment imaging of other anatomic sites confirmed the value of surface dose imaging more broadly.

Corresponding author: Lesley A. Jarvis, MD, PhD; E-mail: lesley.a.jarvis@hitchcock.org

This work has been funded by grant R01 EB023909 from the National Institutes of Health, with hardware support through R44 CA232879 and with the support of the Norris Cotton Cancer Center shared resources in P01 CA023108.

Disclosures: L.A.J. and B.W.P. have a financial interest in DoseOptics, which manufactures cameras used in this study and is funded by SBIR grants; they also have a conflict of interest management plan at Dartmouth College and Dartmouth-Hitchcock Medical Center, which includes an independent review of the research integrity before publication. L.A.J. has a patent pending (application no. 62/874,124). R.L.H. has a patent pending (application no. 62/874,124). M.J. and P.B. are employees of DoseOptics. I.I.T. has a patent issued (WO/2019/165196). M.J. has a patent (WO 2019/143972 A2) pending to Dartmouth/DoseOptics LLC. P.B. has patents pending (62/967,302; 62/873,155; PCT/US19/14242; and PCT/US19/19135). D.J.G. has a patent issued (US10,201,718 B2, 2/12/2019). B.W.P. has patents (US 10201718 B2 and US 9731150 B2) issued to DoseOptics LLC and a patent (WO 2019/143972 A2) pending to Dartmouth/DoseOptics LLC. The remaining authors reported no disclosures or conflicts of interest.

Research data are stored in an institutional repository and will be shared upon request to the corresponding author.

Supplementary material for this article can be found at https://doi.org/10.1016/j.ijrobp.2020.11.013.

Int J Radiation Oncol Biol Phys, Vol. 109, No. 5, pp. 1627–1637, 2021
0360-3016/$ - see front matter
https://doi.org/10.1016/j.ijrobp.2020.11.013

Conclusions: Daily radiation therapy can be imaged routinely via Cherenkov emissions. Both the real-time images and the posttreatment, cumulative images provide surrogate maps of surface dose delivery that can be used for incident discovery and/or continuous improvement in many delivery techniques. In this initial 64-patient cohort, we discovered 6 minor incidents using Cherenkov imaging; these otherwise would have gone undetected. In addition, imaging provides automated, quantitative metrics useful for determining the quality of radiation therapy delivery.

Introduction

Cherenkov imaging is a novel technique that captures light emissions during radiation therapy, allowing for visualization of radiation treatments on the patient, in real-time.[1-3] The current realization of this imaging approach relies on time-gated cameras synchronized to the linear accelerator pulsations to detect the low-level light while largely rejecting the ambient room light.[4] The Cherenkov effect occurs when photon or electron beams interact with tissues[5,6] or even with air at low levels.[7] On the surface of tissue, the light produced shows the treatment-beam shapes, and the intensity produced is in proportion to dose, which are both properties well-suited for verification of treatment delivery.[3,8-10] Cherenkov images can be obtained without additional dose to the patient or additional treatment or setup time, which has advantages for use as a routine, on-patient treatment verification system.[8,10,11] The value of this real-time monitoring was examined in this study, which is, to our knowledge, the first reported large patient-case series with mounted cameras installed in the treatment rooms.

Currently, radiation treatments are verified by pretreatment checks of the treatment plan and standard quality assurance (QA) tests of the linear accelerator function,[12] followed by verification of accurate patient position in relation to the treatment field. The plan, machine, and patient verifications are each typically done before treatment is delivered and often intermittently during the course of therapy. Pretreatment QA involves manual verification of plan parameters on the linear accelerator and confirmation of dose delivery for more complex intensity- modulated radiation therapy (IMRT) plans. Patient position is verified by pretreatment imaging with kV or MV films or with cone beam computed tomography (CT) scans if more detailed anatomy is needed. Patient monitoring also can be performed by surface imaging throughout treatment using optical positioning systems for surface-guided radiation therapy (SGRT). Despite these advanced QA systems, none are currently capable of verifying treatment field delivery, spatial and fractional dose, or the patient's position throughout treatment for every fraction of a radiation course. As modern treatment delivery gravitates toward administering larger doses in fewer fractions or very fast dose rates, the monitoring of the patient position and dose delivery throughout the entire delivery of every treatment becomes more important.[13] Balancing this need with the resources and tools currently available is a common clinical challenge.

The feasibility of clinical Cherenkov imaging has been shown previously[3,10,14-16] through small, single-technique pilot analyses of images. However, the practical utility of imaging in everyday radiation practice has not been prospectively documented in a patient cohort that includes multiple prescribed treatment types. Here, we summarize our experience with an installed Cherenkov imaging system, following 64 patients during their standard prescribed radiation treatments. We report minor incidents discovered and provide examples of images that were clinically informative. For clarity, an incident in this work will be defined by the Radiation Oncology Incident Learning System (RO-ILS), which includes even minor errors that lead to adjustments in treatment.[17] Additionally, the utility of Cherenkov imaging for on-patient treatment verification is examined using cohorts of patient images, evaluated for spatial accuracy. We also describe an approach for routine, in vivo daily dose measurements that can be easily performed with this imaging system.

Materials and Methods

Clinical Cherenkov imaging

A total of 64 patients were imaged using a protocol approved by the Dartmouth Institutional Review Board. Consenting patients received their regular prescribed radiation treatments with between 1 and 14 representative fractions imaged. Disease sites imaged were breast (29), sarcoma/lymphomas (23), head and neck (5), lung (2), pelvis (2), brain (2), and face (1), summarized in Table 1. Treatment techniques used were 3D conformal, including field-in-field breast treatments (33) and craniospinal irradiation (CSI) (1), total skin electron therapy (TSET) (15), arc therapy including volumetric modulated arc therapy (VMAT) and conformal arc treatments (14), and total body irradiation (TBI) (1). Imaging was performed using a remote-triggered, time-gated intensified camera system, C-Dose Research (DoseOptics LLC, Lebanon NH), that was either ceiling or tripod mounted in clinical treatment bunkers. Image acquisition and processing, as used in current treatment setups, have been described previously in detail.[14] Cherenkov images are displayed as pseudocolor maps of light intensity, which correspond to the treatment field.

Radiation therapy treatment

Standard treatment plans were generated using Eclipse treatment planning software (Varian, Palo Alto, CA). Briefly, a field-in-field technique was used for whole breast radiation therapy, and a mono-isocenter technique was used when including the regional lymphatics. Breast patients were set up with AlignRT (Vision RT, London, UK). Supine CSI was planned and verified as previously described.[18,19] Head and neck radiation therapy was planned using volumetric-modulated arc therapy, and TSET was delivered using the 6 dual-field Stanford technique.[20,21] For cases where bolus was prescribed, either standardly used bolus material (Elasto-gel or wet towel) or ClearSight Bolus[22] (Innovative Oncology Solutions, Memphis, TN) was used to allow viewing of the Cherenkov light through the bolus.

Table 1 Disease sites and treatment types

Treatment Site	Treatment Diagnoses	Treatment Types	Patients Imaged, No.
Breast	Malignant neoplasm of the right breast, lymphoma	Whole breast radiation + field-in-field	29
Skin/face	Cutaneous T-cell lymphoma, Kaposi sarcoma	TSET/3D conformal /VMAT	17
Head and neck	Lymphoma, squamous cell carcinoma, Hodgkin lymphoma	VMAT	8
Brain	Meningioma, trigeminal neuralgia	SRS	2
Craniospinal irradiation	Myeloma	Lower spine + upper spine + WB	1
Lung	Small-cell lung cancer	SBRT, VMAT	2
Abdomen	Lymphoma	3D conformal	1
Pelvis	Sarcoma, small-cell carcinoma	VMAT, 3D conformal	2
Total body irradiation	Transplant	Total body irradiation	1
Extremities	Sarcoma	3D conformal	1
			64

Abbreviations: SBRT = stereotactic body radiotherapy; SRS = stereotactic radio surgery; TSET = total skin electron therapy; VMAT = volumetric modulated arc therapy; WB = whole brain.

Scintillator imaging

Custom-machine plastic EJ-212 scintillator disks (Eljen Technology, Sweetwater, TX), 1 mm thick × 15 mm diameter, were attached to the skin surface of patients undergoing TSET or whole breast radiation therapy, and scintillator light output was converted to dose from the images using a computer algorithm as previously described.[23] Scintillation measurements were compared with a standard optically stimulated luminescent dosimeter (OSLD) (nanoDot, Landauer, Inc, Glenwood, IL) and were previously verified to have better than 3% agreement for calibrated dose values.[24]

Data analysis

Analytics applied to breast treatments were computed for Cherenkov light fields recorded between fractions to monitor how day-to-day changes compared with either the first day of treatment or the treatment plan. In both cases, the beam area was segmented using thresholding on cumulative images (all frames summed), either from the treatment plan or the imaged Cherenkov light. The segmentations are compared using mean distance to conformity (MDC), defined as

$$MDC = \frac{\sum_{p \in A \oplus B} \min(d(p, A \cap B)}{n},$$

where MDC is the mean distance to conformity, A and B are 2 segmented regions from 2 images, p represents the pixels in the area of disagreement between A and B, n is the number of pixels in p, and d is the distance in pixels. MDC represents the average distance in pixels in the area of disagreement that the image must be moved to agree.

For field matching analysis, preprocessing for CSI treatments where multiple isocenters were used included using biological fiducial points to coregister and stitch images together. These image transformation matrices were applied to cumulative Cherenkov image fields for coregistration. Field match was assessed using the intersection point of the normalized match profiles. The coefficient of variation (or the standard deviation over the mean value σ/μ) of the match point was computed for the breast patient data set of 12 days. Sample supraclavicular/tangent images from day 1 of treatment are shown in Figure 5.

Results

Cherenkov imaging for visual validation of surface dose and to identify suboptimal treatments

The Cherenkov imaging system displays a live video image of the treatment fields on the patient, which is viewed on a computer monitor at the treatment console. Images can be reviewed in real time by clinical staff at the linear accelerator and can be saved for off-line analysis later. The

Cherenkov images in this study were reviewed by the treating radiation therapists and radiation oncologists to determine what information was of clinical benefit and to identify treatment incidents. First noted was that the images were useful to monitor target and adjacent anatomy to ensure appropriate treatment delivery. Figure 1 shows 4 of 11 imaged fractions of a patient receiving standard whole breast radiation therapy, but the case was challenging because of her limited arm mobility (her arm is positioned down as opposed to over her head). The first panel in Figure 1a shows the treatment plan, rendered from the CT and plan files and translated to the view of the camera. Figure 1h shows a treatment that was delivered with the patient positioned as initially planned during simulation. In contrast, the top 3 panels show treatment days when an otherwise undetectable change in patient positioning resulted in dose on the contralateral breast (Fig. 1b and 1d, arrows) or ipsilateral arm (Fig. 1f, arrow). Optical imaging (AlignRT) was used daily for patient setup and was within the set tolerances on each of these treatment days (Fig. 1, right column; see Fig. E1 for AlignRT data and Cherenkov images for all imaged days and supplementary data in Video E1 for cumulative images from 11 different fractions).

Similarly, 3 additional cases highlighted the utility of visual monitoring of surface dose. First, treatment of extremity sarcomas requires attention to patient positioning and motion during treatment to prevent dose to the contralateral extremity. Six of 25 treatment fractions were imaged of a patient being treated for a soft-tissue sarcoma on the left thigh. Cherenkov imaging confirmed that the right leg did not inadvertently receive dose on these days

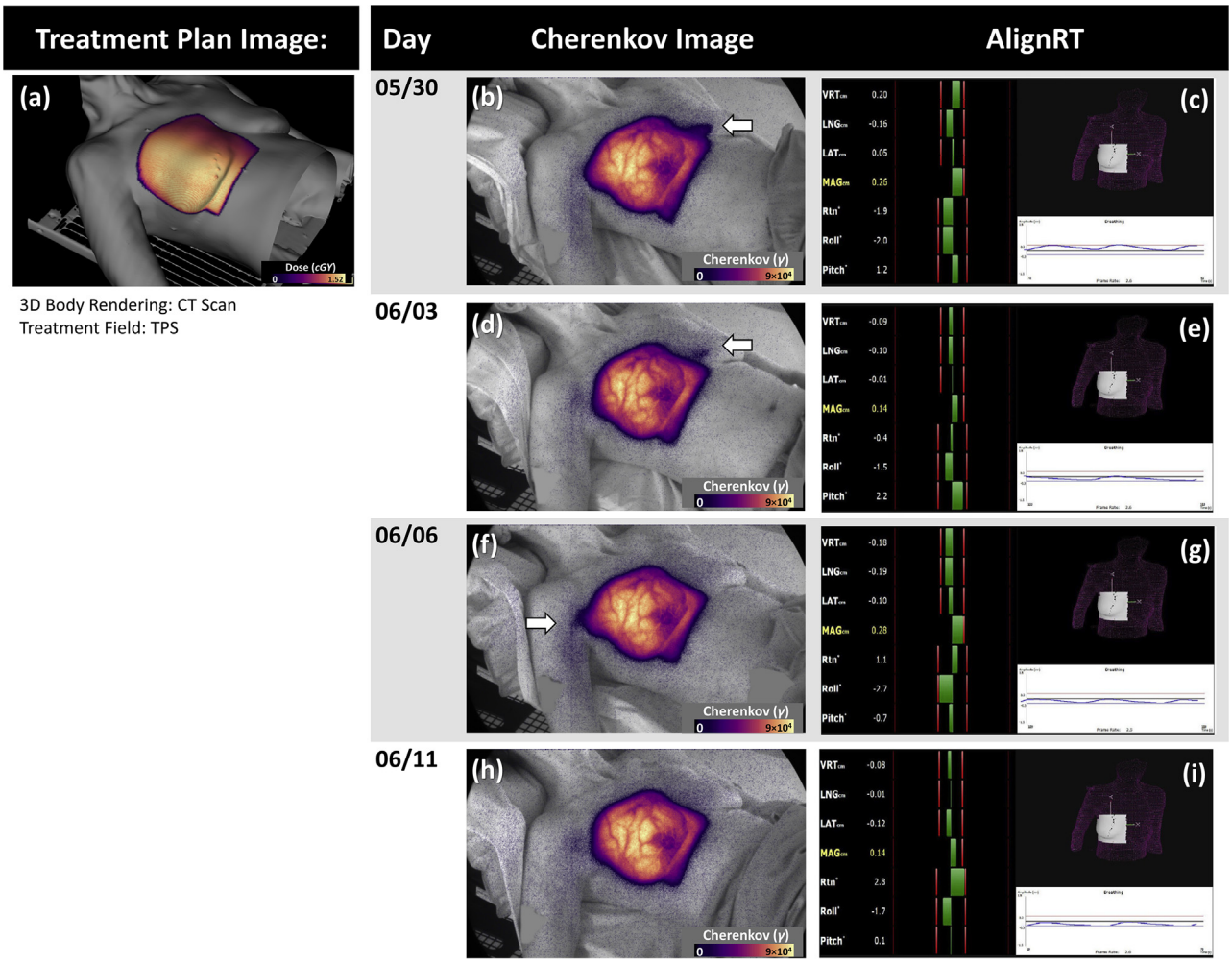

Fig. 1. (a) A visualization of the plan exported from the treatment planning system, rendered onto the patient computed tomography scan surface and shown from the perspective of the Cherenkov camera. Cumulative Cherenkov images are shown from 4 separate fractions, where (h) treatment was executed well relative to the plan; (b) some dose was inadvertently delivered to the contralateral breast; (c) attempts were made to correct the field, although not entirely successful as slight dose was still observable on the contralateral side; and (d) avoiding the left breast was overcompensated for where more dose was delivered onto the arm/shoulder region. The right column shows the corresponding AlignRT screenshots from each day's treatment (c, e, g, and i) with a tolerance margin of ±3 mm.

(see Fig. 2a for a representative fraction imaged). For breast treatments, high tangent fields or supraclavicular fields often treat the low neck while the patient's head is not immobilized. Cherenkov imaging ensured head motion did not result in the chin being inappropriately exposed, for example; Figure 2b shows a high tangent breast plan with delivered dose encroaching on the chin, and Figure 3e and 5e show supraclavicular treatments. This is also important for apical lung treatments, especially pertinent for a patient who was unable to comply with instructions to maintain her head in a still position (see Video E2; the last frame shows the cumulative dose).

Bolus is prescribed to increase surface dose and requires appropriate positioning daily, often precluding physician verification after the initial treatment. In 1 particular case of postmastectomy radiation therapy, bolus was prescribed to cover a large chest-wall treatment area, and 7 of the 28 treatment fractions were imaged using a transparent bolus that allowed for visualization of Cherenkov emissions under the bolus. On 1 of the imaged fractions, the bolus was adequately covering the extent of the left anterior oblique (LAO) treatment field (Fig. 2c, arrow) but not the full medial extent of the right posterior oblique (RPO) treatment field, as demonstrated clearly in the Cherenkov images (Fig. 2d, arrow). There was an additional day when the bolus placement was observed to be close to the field edge in the Cherenkov imaging, with the remaining 5 days of the Cherenkov imaging confirming that the bolus was covering the full treatment fields (data not shown). See Video E3 to observe insufficient bolus coverage on the RPO field from 1 day using a clear bolus.

Finally, detailed review of the Cherenkov video of a field-in-field breast treatment revealed a strip of dose on the inferior breast (Fig. 2f, arrow). The Eclipse treatment plan was investigated, and it was found that the most inferior multileaf collimator (MLC) was inadvertently left open during treatment planning on 1 field-in-field segment because the MLC was immediately adjacent to the inferior jaw and difficult to visualize in all views of the treatment planning system (see Fig. 2e for the field-in-field segment view from the treatment planning system). This was not detected on pretreatment imaging because the combined irradiation aperture outline image does not show field-in-field segments.

Cherenkov imaging to validate spatial accuracy of treatment delivery in breast radiation therapy

To evaluate patient positioning using Cherenkov imaging, 15 breast patients with a total of 129 fractions of imaged treatments were analyzed. These patients were selected because they were imaged with identical camera positions. A general review of the images showed that the captured Cherenkov emissions (Fig. 3a, 3c, 3e, and 3g) qualitatively represented the expected surface dose distribution as predicted by the treatment planning system (compare to Fig. 3b, 3d, 3f, and 3h). This was true for the individual tangent whole breast treatment RPO and LAO fields (Fig. 3a and 3c), for the supraclavicular fields (Fig. 3e), and for a cumulative image of a whole breast plan (Fig. 3g). In addition to validating the field shapes, the Cherenkov images allowed detection of the dose gradients created by the

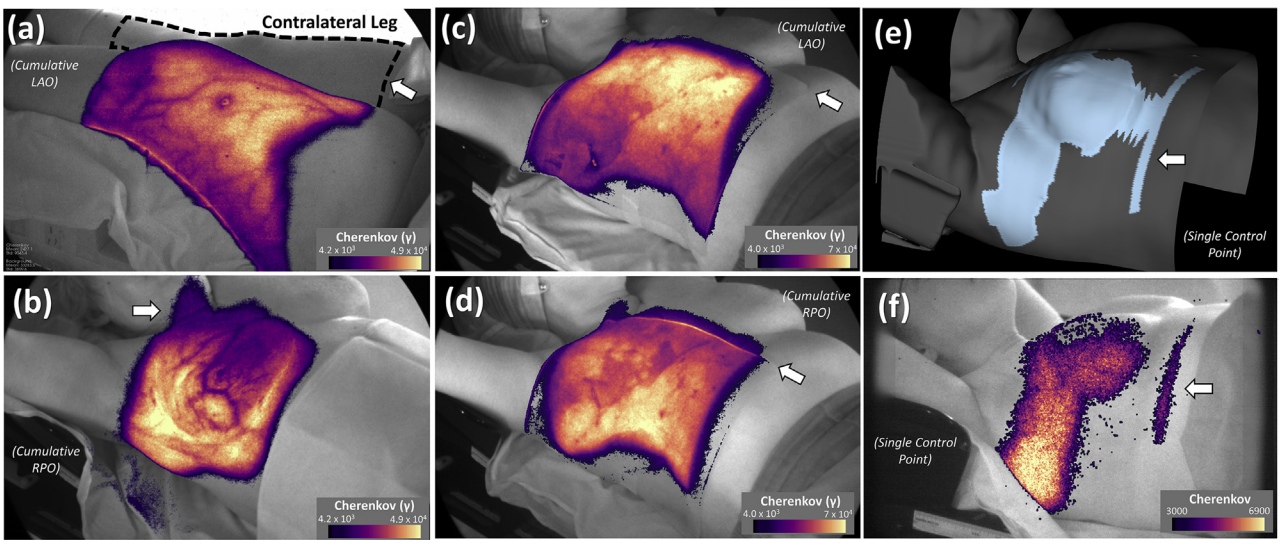

Fig. 2. (a) A leg sarcoma patient was imaged to ensure that the treating beam remained clear of the contralateral leg (a common focus point in the treatment of extremities such as legs). High tangents are another common focus point, shown in (b), where it can be seen if the patient were to move his/her head or chin, which has many degrees of freedom and lacks immobilization. When treating a patient with mastectomy using bolus, accommodating the large field sizes can be difficult, which is shown comparing (c), where the left anterior oblique field was successfully covered with bolus, whereas the right posterior oblique field (d) was not on the medial side. In a less common case, where a multileaf collimator was accidentally left open during planning (e), the Cherenkov image (f) shows this incident very clearly

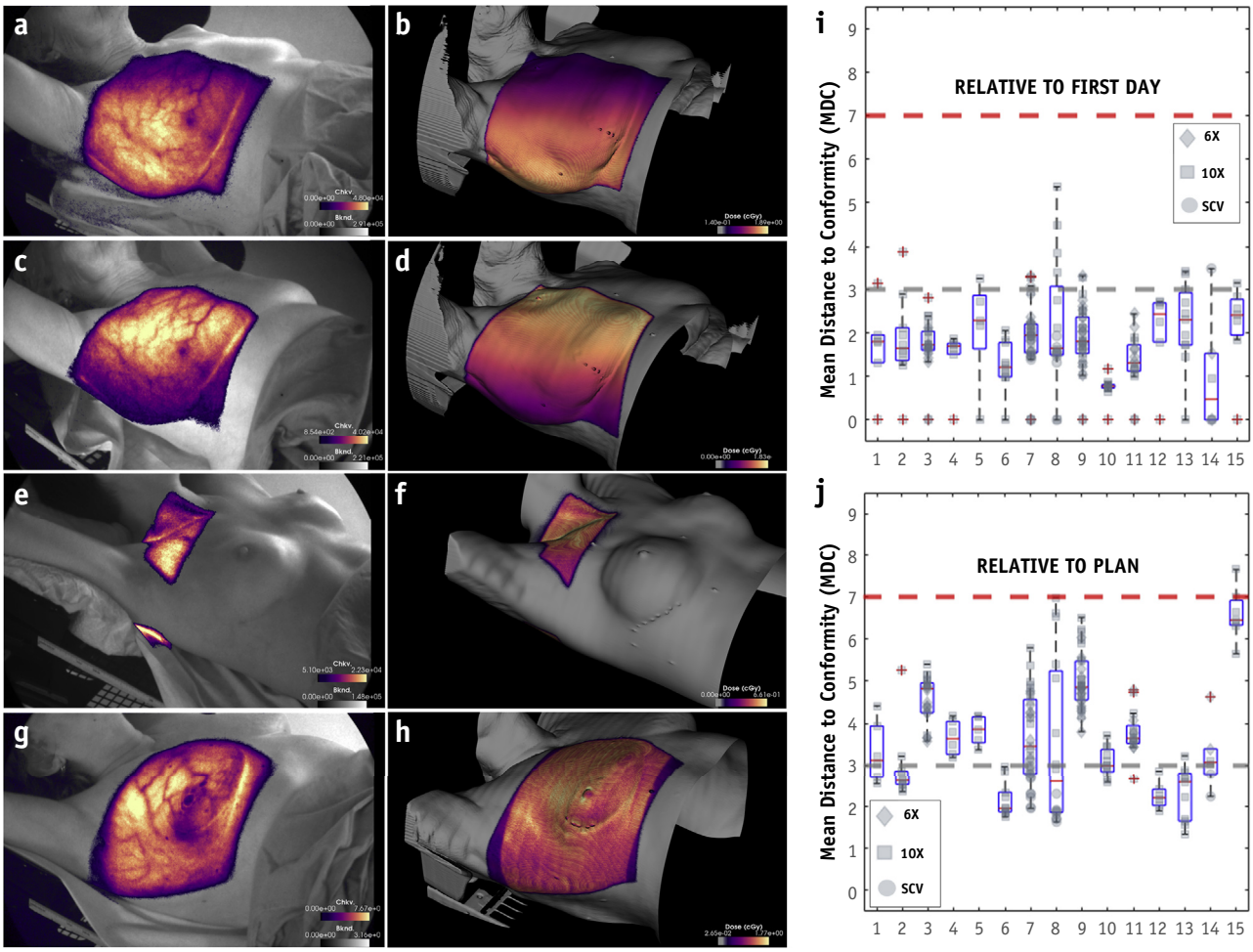

Fig. 3. A sample of a right posterior oblique beam (RPO) Cherenkov image for a patient is shown in (a), which matches the intensity map from the treatment plan (b). The same is shown for the left anterior oblique (LAO) beam (c), which also includes a couch kick, along with its respective cumulative treatment plan image (d). These individual beams illustrate the dose gradient over the surface of the patient, with higher intensity on the entrance side and lower intensity on the exit side, over a gradient. One example of a supraclavicular field is shown in the Cherenkov image (e) and dose image exported from the treatment plan (f). For another patient, the Cherenkov image of cumulative treatment of both LAO and RPO beams (g) is shown matching the cumulative treatment dose image (h). In (i), the mean distance to conformity (MDC) relative to the first recorded treatment day is plotted for all breast patient images, and in (j) this is replotted relative to the treatment plan dose outline as a reference. A dashed gray line indicates where treatment fractions fall within a 3-mm MDC agreement and a red dashed line indicates a 7-mm MDC agreement.

individual tangent beams, as seen in the images for the individual RPO and LAO beams (Fig. 3a, 3b, 3c, and 3d), where the entrance dose and Cherenkov intensity is higher than on the exit side.

The accuracy of treatment delivery was analyzed by calculating the MDC using automated image analysis software built into the Cherenkov imaging system. MDC is calculated as the mean of the root mean squares difference calculated between the measured Cherenkov field edge and either the first day of treatment or the field edge on the surface of the patient CT as defined by the ECLIPSE planning system. Figure 3i shows the MDC for each subsequent fraction compared with the first recorded fraction. Figure 3j compares the MDC for Cherenkov images relative to the Eclipse predicted treatment plan. Compared with the first fraction of breast radiation therapy treatment delivered, no MDC exceeded 7 mm for all 129 averaged RPO/LAO 6X images, for all 49 averaged 10X images, or for 21 supraclavicular treatment images (red dashed line). For stricter 3-mm MDC criteria, it was found that 14 of the 6X images, 3 of the 10X images, and no supraclavicular (SCV) images fell outside this threshold. Compared with the patient treatment plan, higher MDCs were observed. For 6X images, 2 of 129 fell outside the 7-mm criterion, and 85 of 129 fell outside the 3-mm criterion. No SCV or 10X beams exceeded 7 mm, though 47 of 49 10X images and 1 of 21 SCV images exceeded 3 mm.

Cherenkov imaging for on-patient dosimetry

Although Cherenkov light emission is directly proportional to dose in phantoms, the absolute dose cannot be calculated directly from patient images because of variations in tissue optical properties specific to each patient. However, the images do show relative surface dose levels when comparing identical treatment plans delivered to a patient with and without bolus, where the Cherenkov light intensity captured is brighter when the surface dose is higher owing to the presence of bolus (Fig. 4a) compared with a day when bolus was not used (Fig. 4b). To obtain absolute dosimetry with patient Cherenkov imaging, scintillator discs were applied to regions of interest on a patient receiving TSET and 2 patients receiving breast treatment. The surface doses were calculated based on known emission response of the scintillator.[24] Figure 4c shows the surface dose calculated at 5 independent sites simultaneously during delivery of total skin electron beam therapy with scintillator doses in blue and OSLD measured doses in green. Similarly, for breast radiation therapy, surface dose was measured from a scintillator in 2 patients (Fig. 4d and 4e, blue) and compares favorably with OSLD measured doses (green). See Video E4 of a breast treatment with a scintillator in place.

Monitoring of field match lines

Another potential use for Cherenkov imaging is to monitor treatment field match lines[8] so that field junctions are neither overdosed nor underdosed inadvertently. A particularly challenging clinical scenario is verification of matching fields for CSI when the patient is in a supine position, because unlike prone positioning, the gap between the 2 spine fields cannot be visualized directly on the patient.[25] Cherenkov cameras were used to image supine CSI treatments, in particular, to monitor matching field lines on the superficial surface of the patient. Figure 5 shows the treatment plan (a) and Cherenkov images (b, c, and d) for a patient treated with supine CSI using posterior−anterior (PA) upper and lower spine fields as well as whole brain fields registered together. The low-level exit dose from the individual PA spine fields are visible on the patient's abdomen in the Cherenkov images (Fig. 5b, 5c), as well as the dose from the opposed brain fields on the patient's mask and neck (Fig. 5d, cumulative image). For the first match line, the brain fields were set (using couch kicks and collimator angles) at the divergence of the upper spine fields to create an exact match. The Cherenkov image provided a simple visual confirmation that these fields were appropriately aligned (Fig. 5d, arrow). For the second

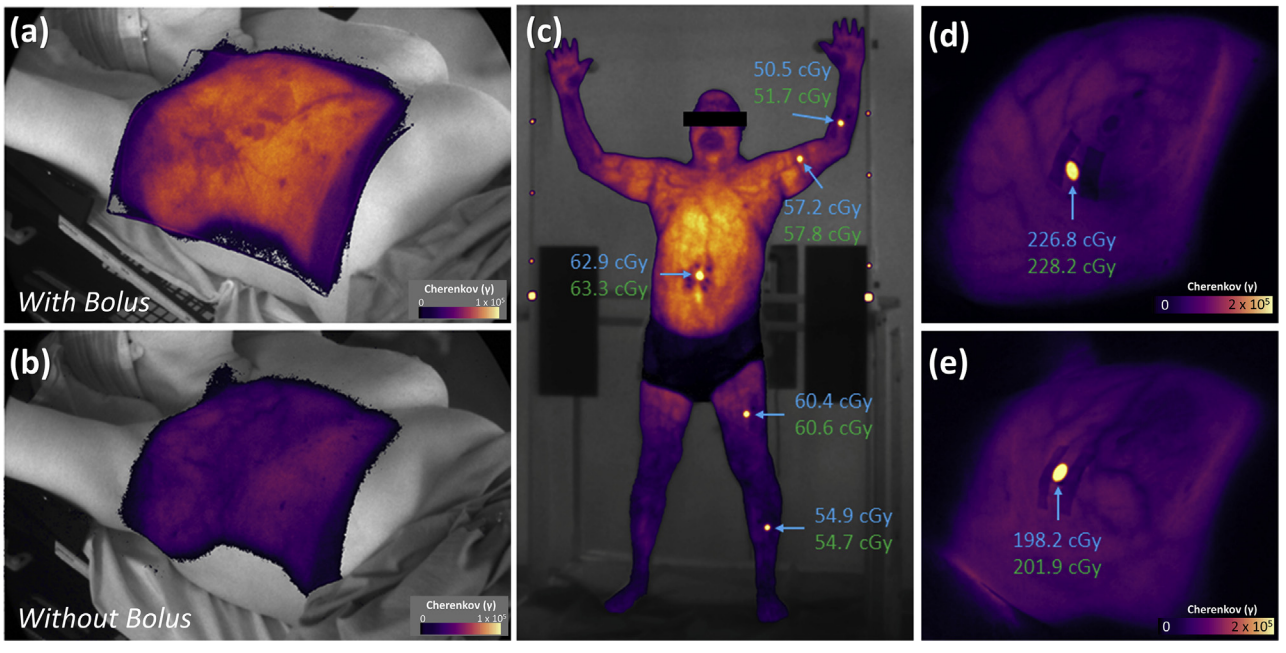

Fig. 4. (a) Cherenkov imaging through clear bolus applied to a breast irradiation case and (b) Cherenkov imaging of the same patient without bolus, showing a lower signal resulting from a lower surface dose. (c) Imaging of a total skin electron therapy patient shows Cherenkov from the skin and scintillation from localized dots placed on the skin, with calculated surface dose values. (d), (e) Surface doses are shown for 2 different whole breast radiation cases were a single scintillating dot was placed on the breast during Cherenkov imaging. Surface dose values from scintillator and optically stimulated luminescent dosimeter are reported in blue and green text, respectively. (A color version of this figure is available at https://doi.org/10.1016/j.ijrobp.2020.11.013.)

match line, the upper and lower spine fields were designed to intersect at the spine, and therefore, there was overlapping dose as each field exited the patient's abdomen (Fig. 5a, white square). This overlap area was visualized on the Cherenkov image (Fig. 5d, white square) and used as an additional means to verify the setup of the spine fields.

A more common scenario for field matching in the clinic is with whole breast tangential fields and supraclavicular fields to treat regional nodes.[26] Cherenkov images of a supraclavicular field (Fig. 5e), the whole breast fields (Fig. 5f), and the cumulative combined image (Fig. 5g) are shown. The Cherenkov images were analyzed to determine daily accuracy of the match using C-Dose software.[16,17] For the breast treatment shown in Figure 5, the match profiles were analyzed, and consistency (coefficient of variation) was found to fall within 3.7% for 13 acquisitions. See Video E5 of an entire treatment for a patient with a field match breast and SCV treatment.

Discussion

Radiation therapy is known to be safe, but clinically significant errors do happen, as well as more common, minor incidents that are of lower clinical significance.[27,28] In addition, RO-ILS has reported that the majority of radiation incidents are identified during treatment delivery and discovered by therapists.[17] As such, we hypothesized that if radiation treatments could be "seen," that is,

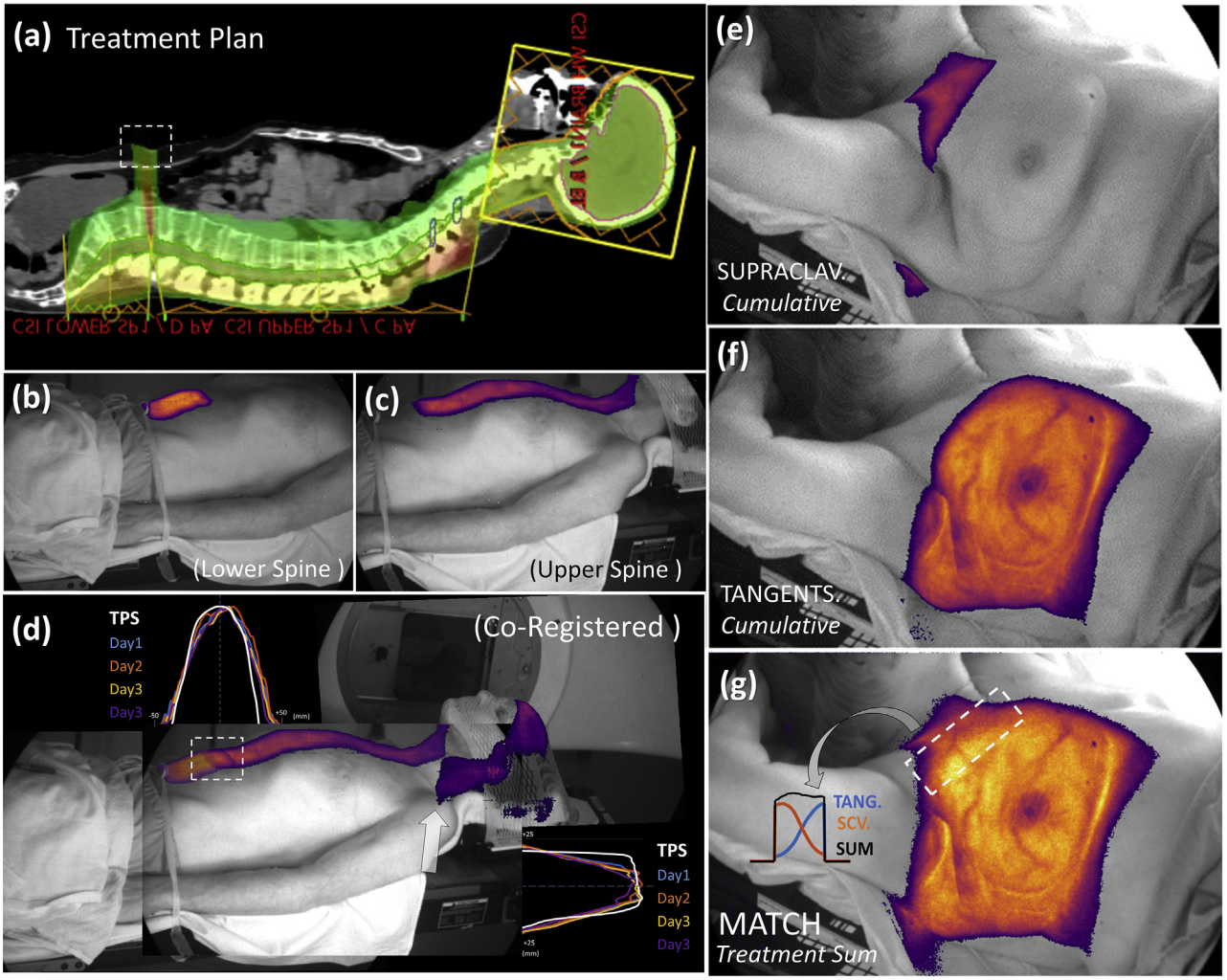

Fig. 5. (a) A treatment plan for cerebral-spinal irradiation, characterized by 4 fields and 3 isocenters: a right and left lateral whole brain field, an upper spine field, and a lower spine field. A technique for stitching together the Cherenkov treatment images was developed by first isolating the lower spine field individually (b) and then the upper spine (c). The result (d) shows the sum, with biological fiducials used to register the background and Cherenkov images together; profiles comparing days 1 through 4 of lower and upper spine junction areas are shown, as compared with what was seen in the treatment plan. (e) The supraclavicular cumulative fields treating the axial nodes of a patient. (f) The 4 tangent beam images (left anterior oblique / right posterior oblique 6X/10X) summed together are added with the supraclavicular field (g). The match region has a bounding box that isolates the profile intersection region, such that the meeting of the 2 beams can be analyzed.

visualized in real-time by the treatment team at the console, there would be opportunities to improve therapy through detection of unforeseen issues. In this first cohort of 64 patients, we identified several general scenarios where viewing Cherenkov imaging provided useful information:

1. Evaluating patient setup. We reported fractions where Cherenkov imaging identified unintended dose on adjacent anatomy. There are several sites where it is important to avoid treating adjacent normal anatomy, including breast treatments (arm, chin, contralateral breast), extremity treatments (contralateral leg), and face treatments (eye).[29] It is likely that this type of incident will be detected more commonly in patients with difficult setups owing to physical constraints in mobility (such as the patient shown in Fig. 1) or with a challenging body habitus (such as patients with large, pendulous breasts). In addition to monitoring adjacent anatomy, the Cherenkov imaging also shows treatment fields with respect to pertinent at-risk anatomy (eg, scars) and ensures bolus is positioned adequately to cover the target area.

2. Monitoring patient compliance. When patients move during treatment delivery, it is often not detected, or the consequence of the movement is not known. The Cherenkov images are a video recording of the beam interacting with the patient's surface (see supplemental videos), providing a record of the daily treatment that can be evaluated in real time or saved for documentation and review at a later date. Positional changes during beam delivery are important for patients who have difficulty maintaining the prescribed treatment position because of pain or altered mental status. In cases where there is significant movement during treatment, the Cherenkov video can be reviewed and estimation of change in delivered dose can be made.

3. Identifying machine or plan issues. Cherenkov imaging visualizes the final step in the complex process of treatment planning and delivery. As such, it is a final check of the process by showing the field shape on the patient is as expected. We show the sensitivity of this imaging to detect even a single MLC position during delivery of 1 field-in-field segment as being in a position that was not intended. Because this imaging can be performed daily, it has the potential to detect small changes that could be introduced with plan revisions, faulty equipment, or changes to the patient anatomy during the course of treatment.

In this small sample of patients, we observed 6 patient treatment courses for which the in vivo, real-time Cherenkov imaging provided valuable insight to the delivery team. It is important to note that all patients in this study were set up with standard techniques including tattoos, port films, kV imaging, cone beam CT, or AlignRT, depending on the treatment site. For example, we identified breast patients with positioning issues detected by Cherenkov imaging, even though these patients had been set up with an optical positioning system (AlignRT) that reported positioning within the set tolerance levels. This incongruity may happen because tolerances are not stringent enough to prevent the dose spill that was found. Importantly, Cherenkov imaging has the ability to visually show the consequence, in terms of a change in surface dose, of inaccuracies or compromises made during patient positioning. Typical regions of interest (ROIs) for surface optical imaging systems are often focused on a small area and do not detect alignment issues outside of the ROI. This may have the consequence of giving the clinical team a false sense of security in reference to anatomy outside of the ROI, where there could be stray beam. Adding Cherenkov imaging to a surface optical imaging system would be ideal for on-patient verification, as it not only could provide positional monitoring in and outside of the ROI but also could reveal beam-related issues during the critical time of treatment beam delivery.

In addition to the real-time view of radiation, Cherenkov images can be analyzed later to evaluate accuracy or dosimetry. Importantly, the system can remain on and is simply a remote camera that adds no extra time or dose to the patient. The analysis can be automated, so large-scale review of treatment repeatability in a clinic is possible through centralization of the data files. For analysis of positional precision and accuracy, these number sets can indicate a patient who is difficult to set up, for example, and who might require different immobilization. These metrics also could be valuable to assess procedural changes and impact on treatment delivery (ie, switching from tattoos/lasers to AlignRT for breast treatments). For dosimetry, the system can also be automated to identify the scintillators in the image and convert the intensity to dose, allowing multiple sites to be sampled on a daily basis without the time-consuming steps required for processing thermoluminescent diodes (TLDs) or reading out OSLDs. Without scintillators, uncompensated emissions cannot substitute for absolute dose measurements on the surface. However recently published work[30] has used tissue density from CT images to more closely correlate Cherenkov light intensity to dose ($\pm$10%), and more work continues to implement these tissue optical property corrections.

Overall, Cherenkov imaging provides a valuable noninvasive means to routinely monitor and improve the quality of daily treatment. The images can be viewed at the treatment console or at a remote computer, allowing an unprecedented ability to visually evaluate treatment delivery in real time by the radiation therapists but also by the radiation oncologist and/or a physics team remote from the treatment machine. Future work will be needed to fully analyze the most complex treatments, such as those used in head and neck cancer treatment (see Video E6 to view a head and neck treatment that shows a dual-camera setup used to circumvent gantry blockage during VMAT).

The clinical significance of the individual incidents and cases in this study were minor, but even in this limited cohort, we found opportunities to improve treatment delivery for individual patients. Of specific clinical importance, we show that Cherenkov imaging can detect stray radiation dose to tissues. Currently, there is no practical technique available to monitor contralateral breast dose or dose to other adjacent anatomy on a daily basis. Other measurement techniques, such as TLDs or OSLDs, are limited to point measurement and are resource intensive for routine use, and it is currently impossible to accurately predict a spatial area of concern to guide TLD/OSLD placement. For breast patients, it is well documented that women who have had breast cancer are 2.5 times as likely to have secondary breast cancer, and an appreciable fraction of these patients will develop a new cancer in the contralateral breast because of the radiation dose during treatment.[31] The risk is directly proportional to the dose to the breast and inversely proportional to the patient's age. A large study of secondary breast cancer by Burt et al[32] showed that approximately 3.4% of patients receiving breast radiation therapy had additional cancer attributable to the radiation, with a relative risk ratio of 1.33 for the radiation therapy cases relative to 1.2 for the control, although this range is known to be closer to 1.59-1.32 for younger women. It is widely accepted that additional dose to the contralateral breast can lead to cancer, especially in young women; therefore, great effort is made at the treatment-planning steps to minimize contralateral breast dose. However, as we have shown in this relatively small cohort, patient misalignment or patient movement during treatment can lead to increased contralateral breast dose despite good treatment-planning technique and use of SGRT. To date, technology has not existed to monitor contralateral breast dose on a daily basis to ensure dose to the contralateral breast does not exceed the planned dose.

We anticipate that an "always on" system, used to monitor all patient treatments in a clinic, would give valuable information about treatment delivery at approximately the rate that we detected in this cohort (6 of roughly 343 fractions, or approximately 1.7% of treatments), as well as being able to detect more significant incidents at a time when the treatment can be altered or aborted. Importantly, this work justifies proceeding with a large, multicenter trial designed to evaluate minor and major incidences in routine clinical practice using this noninvasive and intuitive imaging technique.

Conclusions

The 64 patients imaged to date show the value of Cherenkov imaging as a tool for treatment validation. The imaging of all patients over a range of techniques provided several observations of incidents in which there was suboptimal delivery, and importantly, it demonstrated the potential value for an intuitive daily view of every patient's treatment, which has never been possible before in radiation therapy. The imaging provides a visualization of the treatment beam on the patient's skin, bolus, or mask, which could be used subsequently to identify ways to optimize treatment delivery. Future goals to use large-scale clinical imaging could help determine whether more or more significant incidents are detected, and more importantly, corrected to improve the overall quality of day-to-day treatments.

References

1. Steidley KD, Eastman RM, Stabile RJ. Observations of visual sensations produced by Cerenkov radiation from high-energy electrons. *Int J Radiat Oncol Biol Phys* 1989;17:685-690.
2. Newman F, Asadi-Zeydabadi M, Durairaj VD, Ding M, Stuhr K, Kavanagh B. Visual sensations during megavoltage radiotherapy to the orbit attributable to Cherenkov radiation. *Med Phys* 2008;35:77-80.
3. Jarvis LA, Zhang R, Gladstone DJ, et al. Cherenkov video imaging allows for the first visualization of radiation therapy in real time. *Int J Radiat Oncol Biol Phys* 2014;89:615-622.
4. Andreozzi JM, Zhang R, Glaser AK, Jarvis LA, Pogue BW, Gladstone J. Camera selection for real-time in vivo radiation treatment verification systems using Cherenkov imaging. *Med Phys* 2015;42:994-1004.
5. Čerenkov P. Visible radiation produced by electrons moving in a medium with velocities exceeding that of light. *Phys Rev* 1937;52:378.
6. Blumenthal DT, Corn BW, Shtraus N. Flashes of light-radiation therapy to the brain. *Radiother Oncol* 2015;116:331-333.
7. Fahimian B, Ceballos A, Turkcan S, Kapp DS, Pratx G. Seeing the invisible: Direct visualization of therapeutic radiation beams using air scintillation. *Med Phys* 2014;41:010702.
8. Black PJ, Velten C, Wang YF, Na YH, Wuu CS. An investigation of clinical treatment field delivery verification using Cherenkov imaging: IMRT positioning shifts and field matching. *Med Phys* 2019;46:302-317.
9. Roussakis Y, Zhang R, Heyes G, et al. Real-time Cherenkov emission portal imaging during CyberKnife(R) radiotherapy. *Phys Med Biol* 2015;60(22):N419-N425.
10. Zhang R, Andreozzi JM, Gladstone DJ, et al. Cherenkoscopy based patient positioning validation and movement tracking during post-lumpectomy whole breast radiation therapy. *Phys Med Biol* 2015;60:L1-L14.
11. Miao T, Bruza P, Pogue BW, et al. Cherenkov imaging for linac beam shape analysis as a remote electronic quality assessment verification tool. *Med Phys* 2019;46:811-821.
12. AAPM Medical Physics Practice Guideline 5.a.: Commissioning and QA of treatment planning dose calculations—Megavoltage photon and electron beams. *J Appl Clin Med Phys* 2016;17:457.
13. Ford E, Deye J. Current instrumentation and technologies in modern radiobiology research—Opportunities and challenges. *Semin Radiat Oncol* 2016;26:349-355.
14. Hachadorian R, Bruza P, Jermyn M, et al. Correcting Cherenkov light attenuation in tissue using spatial frequency domain imaging for quantitative surface dosimetry during whole breast radiation therapy. *J Biomed Opt* 2018;24:1-10.
15. Xie Y, Petroccia H, Maity A, et al. Cherenkov imaging for total skin electron therapy (TSET). *Med Phys* 2020;7:201-212.
16. Zhang R, Gladstone DJ, Jarvis LA, et al. Real-time in vivo Cherenkoscopy imaging during external beam radiation therapy. *J Biomed Opt* 2013;18:110504.
17. Evans SB. First fruits of the RO-ILS system: Are we learning anything new? *Pract Radiat Oncol* 2018;8:133-135.

18. Michalski JM, Klein EE, Gerber R. Method to plan, administer, and verify supine craniospinal irradiation. *J Appl Clin Med Phys* 2002;3:310-316.
19. McMahon RL, Larrier NA, Wu QJ. An image-guided technique for planning and verification of supine craniospinal irradiation. *J Appl Clin Med Phys* 2011;12:3310.
20. Chen Z, Agostinelli AG, Wilson LD, Nath R. Matching the dosimetry characteristics of a dual-field Stanford technique to a customized single-field Stanford technique for total skin electron therapy. *Int J Radiat Oncol Biol Phys* 2004;59:872-885.
21. Gamble LM, Farrell TJ, Jones GW, Hayward JE. Composite depth dose measurement for total skin electron (TSE) treatments using radiochromic film. *Phys Med Biol* 2003;48:891-898.
22. Adamson JD, Cooney T, Demehri F, et al. Characterization of water-clear polymeric gels for use as radiotherapy bolus. *Technol Cancer Res Treat* 2017;16:923-929.
23. Bruza P, Gollub SL, Andreozzi JM, et al. Time-gated scintillator imaging for real-time optical surface dosimetry in total skin electron therapy. *Phys Med Biol* 2018;63:095009.
24. Tendler I, Bruza P, Andreozzi J, et al. Rapid multi-site remote surface dosimetry for total skin electron therapy: Scintillator target imaging. *Int J Radiat Oncol Biol Phys* November 9, 2018.
25. Hachadorian RL, Jarvis LA, Gladstone DJ, Jermyn M, Bruza P, Pogue BW. Using Cherenkov imaging to assess field overlap in cranial-spinal irradiation (CSI). *Int J Radiat Oncol Biol Phys* 2019;105:E729-E730.
26. Garg AK, Frija EK, Sun TL, et al. Effects of variable placement of superior tangential/supraclavicular match line on dosimetric coverage of level III axilla/axillary apex in patients treated with breast and supraclavicular radiotherapy. *Int J Radiat Oncol Biol Phys* 2009;73:370-374.
27. Spraker MB, Fain R III, Gopan O, et al. Evaluation of near-miss and adverse events in radiation oncology using a comprehensive causal factor taxonomy. *Pract Radiat Oncol* 2017;7:346-353.
28. Hoopes DJ, Dicker AP, Eads NL, et al. RO-ILS: Radiation oncology incident learning system: A report from the first year of experience. *Pract Radiat Oncol* 2015;5:312-318.
29. Tendler II, Hartford A, Jermyn M, et al. Experimentally observed Cherenkov light generation in the eye during radiation therapy. *Int J Radiat Oncol Biol Phys* 2020;106:422-429.
30. Hachadorian RL, Bruza P, Jermyn M, et al. Imaging radiation dose in breast radiotherapy by X-ray CT calibration of Cherenkov light. *Nat Commun* 2020;11:2298.
31. Stovall M, Smith SA, Langholz BM, et al., Women's Environmental, Cancer, and Radiation Epidemiology Study Collaborative Group. Dose to the contralateral breast from radiotherapy and risk of second primary breast cancer in the WECARE study. *Int J Radiat Oncol Biol Phys* 2008;72:1021-1030.
32. Burt LM, Ying J, Poppe MM, Suneja G, Gaffney DK. Risk of secondary malignancies after radiation therapy for breast cancer: Comprehensive results. *Breast* 2017;35:122-129.